Dioxatriazamacrocycle-*N*,*N*′,*N*″-triacetic Acids: Synthesis, Protonation Constants, and Metal-Complex Studies. Crystal Structure of Hydrogen [1,4-Dioxa-7,10,13-triazacyclopentadecane-7,10,13-triacetato(4)-κN^7,κN^{11},κN^{13},κO^7]copper(1–) Hydrate (2:1) ([Cu(HL^1)]·0.5 H_2O)

by **M. Fátima Cabral**[a][b], **Rita Delgado**[a][c]*, **M. Teresa Duarte**[c], and **Miguel Teixeira**[a]

[a]) Instituto de Tecnologia Química e Biológica, UNL, Apartado 127, P-2781-901 Oeiras
[b]) Faculdade de Farmácia de Lisboa, Av. das Forças Armadas, P-1600 Lisboa
[c]) Instituto Superior Técnico, Av. Rovisco Pais, P-1049-001 Lisboa

Two new dioxatriazacyclopentadecanetriacetic acids were synthesized, *i.e.* 1,4-dioxa-7,10,13-triazacyclopentadecane-7,10,13-triacetic acid (**1**; H_3L^1) and 1,4-dioxa-7,10,14-triazacyclohexadecane-7,10,14-triacetic acid (**2**; H_3L^2). The protonation constants of these compounds and the stability constants of complexes of both ligands with the alkaline-earth metal ions, Mn^{2+} to Zn^{2+}, Cd^{2+}, and Pb^{2+} were determined by potentiometric methods at 25° in 0.10M tetramethylammonium nitrate solution. Both ligands exhibit two high-value protonation constants and two low-value ones. Only mononuclear complexes were found for both ligands with the alkaline earth metal ions, and their stability constants are surprisingly low, suggesting the involvement of only two N-atoms of the macrocycles and two carboxylate groups in the coordination to these metal ions (or a very weak interaction with all the carboxylates). Mono- and dinuclear species were found in solution for most of the divalent first-row transition-metal ions, Cd^{2+}, and Pb^{2+}. Ligand **1** (H_3L^1) formed mononuclear complexes that were thermodynamically more stable, while **2** (H_3L^2) stabilized the dinuclear species better due to the larger cavity size of the macrocycle. Electronic and EPR-spectroscopic studies in solution revealed that the Co^{2+}, Ni^{2+}, and Cu^{2+} complexes are six-coordinate, and that the three N-atoms of the macrocycles are involved in the coordination. EPR Spectra of the copper(II) dimer of **2** show resonances corresponding to the $\Delta M_s = 1$ and $\Delta M_s = 2$ transitions. The structure of [Cu(HL^1)]·0.5 H_2O, obtained from Cu^{2+} and **1**, was determined by single-crystal X-ray diffraction. The complex adopts a distorted compressed trigonal-bipyramidal geometry, with the macrocycle in a folded conformation. The basal plane is formed by two N- and one O-atoms of the macrocycle backbone, and the apical positions are occupied by the other N-atom of the ring and one of the O-atoms of one carboxylate group. Electronic and EPR-spectroscopic studies show that the same complex exists in solution in a six-coordination symmetry with tetragonal elongation.

1. Introduction. – Most of the published coordination chemistry of macrocyclic compounds involves crown ethers and cyclic amines [1–3]. Much less work has been done with mixed macrocyclic ligands containing O- and N-donors, and the pentadentate ligands are among the least studied [1–4]. We have now synthesized the two new pentadentate macrocycles **1** (H_3L^1) and **2** (H_3L^2) containing N- and O-atoms as donor atoms and acetic acid pendant arms, which are potential eight-coordinate ligands with a N_3O_5 coordination sphere. In the present work, we studied the acid-base equilibrium reactions of both ligands and some of their metal complexes.

The size of the cavity of a 15-membered macrocycle is sufficiently large to accommodate most of the metal ions studied in this work. However, in the complex [CuL^4]·$(H_2O)_2$, where H_2L^4 is 1,4,10-trioxa-7,13-diazacyclopentadecane-7,13-diacetic acid (**4**), which is also a 15-membered macrocycle with acetic-acid arms and five donor atoms in the ring, the Cu^{2+} ion is completely encapsulated in the macrocycle and

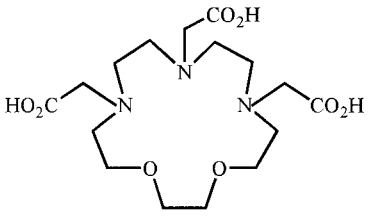

1 H_3L^1

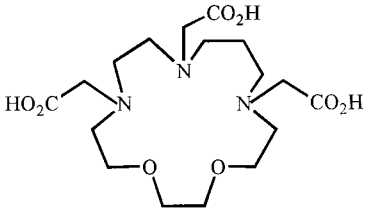

2 H_3L^2

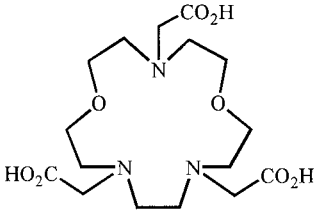

3 H_3L^3

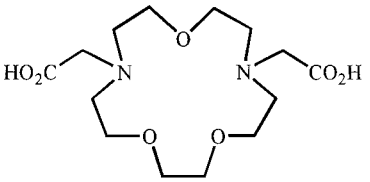

4 H_2L^4

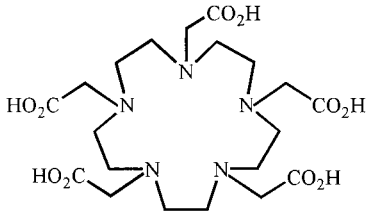

5 H_5L^5

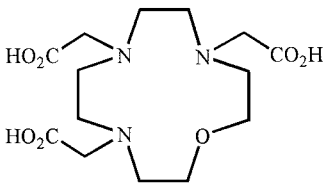

6 H_3L^6

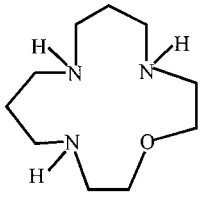

7 L^7

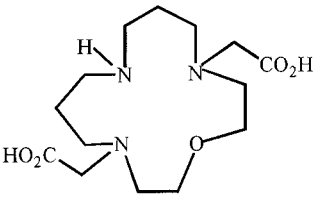

8 H_2L^8

coordinates to all donors of the ring which constitute the equatorial plane of a distorted compressed pentagonal bipyramid, the O-atoms of the acetic-acid arms being in the axial positions. The Cu^{2+} ion fits well in the cavity of the macrocycle and is displaced only by 0.02(2) Å above the least-square equatorial plane [5][6]. Crown ethers of the type [15]crown-O_5 also form Cu^{2+} complexes, with the metal ion in a similar compressed pentagonal-bipyramidal geometry [7][8]. Due to the adopted geometry, the thermodynamic stability constant of $[CuL^4]$ is relatively high [9]. Therefore, as

ligand **1** has an N-atom with an acetic-acid arm replacing an O-atom of the ring of **4** (H_2L^4), we expected complexes having high thermodynamic stability. But our expectations were not completely fulfilled. Additionally, the free donor atoms of **1** and **2** can coordinate to another metal ion forming dimeric or polymeric species. Indeed, dimeric complexes were found in solution, especially with the 16-membered macrocycle **2**.

2. Results and Discussion. – 2.1. *Acid-Base Equilibrium Reactions.* In *Table 1*, the protonation constants of both ligands **1** and **2** and also of other similar compounds are collected. Both macrocycles exhibit two high-value protonation constants and two low-value ones. The higher values are similar to the corresponding constants of the parent macrocycles [10] and also to other N_xO_y macrocycles of the same size, such as **3** (H_3L^3) [11] and **4** (H_2L^4) [9a]. The first two protonations of **1** and **2** occur at amine centers, the second one at the amine center located at a greater distance from the first already protonated to minimize the charge repulsion. These constants, as well as those of all the other N_xO_y macrocycles, are lower than the corresponding values of similar compounds having the same size but only N-donors in the ring as shown, for instance, by a comparison of the values for the 15-membered compounds **1**, **3**, and **4** (*Table 1*) with those of the pentaazamacrocycle **5** (H_5L^5; log $K_1 = 10.15$ and log $K_2 = 9.41$, at 25° and $I = 0.20$M in $NaNO_3$) [12]; similarly, the values of the tetraazamacrocycles [13] are higher than those of the oxatriaza- [14] or of the dioxadiazamacrocycles [15]. This effect becomes less pronounced with the increase of the cavity size of the macrocycle and is in part explained by the electron-withdrawing effect of the nearby O-atoms.

Table 1. *Protonation* (log K_i^H) *Constants of* **1** (H_3L^1), **2** (H_3L^2), *and Other Similar Ligands for Comparison.* $T = 25.0°$; $I = 0.10$M in $(Me_4N)NO_3$.

Equilibrium quotient	**1** (H_3L^1)	**2** (H_3L^2)	**3** (H_3L^3)[a])	**4** (H_2L^4)[b])	**6** (H_3L^6)[c])
$[HL]/[H]\cdot[L]$	10.02(1)	9.77(2)	9.55	9.067	11.61
$[H_2L]/[HL]\cdot[H]$	7.93(2)	8.11(2)	8.92	8.544	7.70
$[H_3L]/[H_2L]\cdot[H]$	3.93(3)	4.12(3)	4.51	1.75	4.05
$[H_4L]/[H_3L]\cdot[H]$	2.41(5)	1.84(4)	1.59	< 1	2.77
$[H_4L]/[L]\cdot[H]^4$	24.29	23.84	24.57	< 20.4	26.13

[a]) $I = 0.10$M in KCl [11]. [b]) [9a]. [c]) [14].

The higher values found for the first protonation constant of macrocycles having only N-donors in the ring when compared with noncyclic compounds of the same type are generally attributed to the formation of internal H-bonds of the type $N-H\cdots N$ within the ring, which will stabilize the protonated form, or to the higher electron density in the macrocyclic cavity when the nonbonded electron pairs of the amine N-atom are directed towards the center of the ring [4][16]. Both explanations are more adequate for small cavity sizes, *i.e.* for 9- to 13-membered macrocycles. So it is not surprising that the increase of the size of the cavity leads to values of the first protonation closer to those of noncyclic amines. *Hancock* and co-workers. [16] have verified that the basicities of noncyclic triamines (K_1^H and K_2^H) are not markedly electronically influenced when the central N-atom is replaced by other atoms, such as O or S, and likewise macrocycles having three donors of the type N_2O and N_2S exhibit

similar behavior. Hence they have concluded that the values for the first protonation of N_2X macrocycles (X being N, O or S) are in conformity with the internal H-bonding model, and run parallel to the H-bonding ability $N \gg O > S$ of the central donor atom [16]. However, the H-bonding ability of $N-H\cdots X$ runs parallel to the electronegativity of X, being higher for $N-H\cdots O$ than for $N-H\cdots N$, and so we would expect higher protonation constants for amines of macrocycles containing also O donor atoms. But the experimental results suggest the opposite. Thus, one should consider additional factors for the interpretation of these values, such as the conformational rearrangement of the macrocycle. The direction of the lone pairs of X depends on this rearrangement, and they can point towards the inside or the outside of the ring. The single lone pair of N-atoms can be more easily directed to the cavity for small ring sizes, and in the correct direction for the maximum interaction with the H-atom for the formation of H-bonding, as compared with the two lone pairs of the O-atom. However, because X-ray structures that could clarify this point are missing [4], theoretical studies that probably could shed some light are in progress.

The log value of the third protonation constant of **1** and **2** is *ca.* 4. It can be ascribed either to the protonation of the third amine or to the carboxylate group bound to the nonprotonated amine between the two ammonium groups of both molecules [17]. The parent macrocyclic amines have lower log K_3^H values (2.30 and 4.06, resp. [10]) than **1**, and **2** especially lower than **1**. A ^{1}H-NMR titration of **3** [11] has revealed that the value of 4.51 determined for this ligand corresponds to the protonation of the third amine group, but this compound has an ammonium ion between two O-donors, and, therefore, the repulsion between the three protonated N-atoms is less strong than in our case where the three N-atoms are adjacent. That this value is higher for **2** supports the hypothesis of protonation at the third N-atom.

The fourth protonation of **1** and **2** occurs at the carboxylate groups bound to ammonium ions, as the values are in a typical range for such protonations [14][15][17].

The overall basicity of both compounds is *ca.* 24 in log units, which is the expected value for N_3O_2 macrocyclic complexones, much lower than the value of *ca.* 30 exhibited by most of the tetraaza- and pentaazamacrocycles having *N*-acetic-acid pendant arms.

2.2. *Stability Constants.* The stability constants of **1** and **2** with alkaline earth metal ions, the first-row transition divalent metal ions, Cd^{2+}, and Pb^{2+} are collected in *Tables 2* and *3*, respectively, together with the corresponding known constants of complexes of other macrocycles. Only mononuclear complexes were found for both ligands with the alkaline earth metal ions (*Table 2*), while for the majority of the others (*Table 3*), also dinuclear ones were formed. Indeed, the ligands provide an average number of four atoms for a metal ion in a dimeric complex, which is insufficient for the alkaline earth metal ions, which usually prefer higher coordination numbers (except Mg^{2+} for which the most common coordination number is 6).

2.3. *Complexes of the Alkaline Earth Metal Ions.* It is interesting to stress the low value of stability constants of the complexes of **1** and **2** and also of all the ligands **4** and **5** having the same cavity size (*Table 2*). These ligands exhibit stability constants lower than those of H_4edta (ethane-1,2-diyldinitrilo)tetraacetic acid) and H_4egta ([ethane-1,2-diylbis(oxyethane-1,2-diylnitrilo)]tetraacetic acid). An abrupt decrease of stability constants is also observed when the complexes of **6** (H_3L^6) are compared with those of **1** (even when the differences in basicity are taken into account). It is reported that all

Table 2. *Stability Constants* (log units) *of Alkaline Earth Metal Complexes with* **1** (H_3L^1), **2** (H_3L^2), *and Other Similar Ligands for Comparison.* $T = 25.0°$; $I = 0.10$M in $(Me_4N)NO_3$.

	Equilibrium quotient	**1** (H_3L^1)	**2** (H_3L^2)	**4** (H_2L^4)[a]	**5** (H_5L^5)	**6** (H_3L^6)[b]
Mg^{2+}	[ML]/[M]·[L]	7.34(2)	3.46(5)	7.534	5.0[c])	10.25
	[MHL]/[ML]·[H]	–	–	–	–	5.67
Ca^{2+}	[ML]/[M]·[L]	8.51(1)	7.23(5)	8.680	8.7[c])	12.98
	[MHL]/[ML]·[H]	–	–	–	–	3.93
	[ML]/[MLOH]·[H]	–	(9.7)	–	–	–
Sr^{2+}	[ML]/[M]·[L]	8.09(1)	4.39(3)	8.023	7.31[d]); 9.1[c])	11.37
	[MHL]/[ML]·[H]	–	–	–	–	4.72
	[ML]/[MLOH]·[H]	10.4(1)	–	–	–	–
Ba^{2+}	[ML]/[M]·[L]	7.25(2)	4.06(5)	7.412	–	9.92
	[MHL]/[ML]·[H]	–	–	–	–	6.04
	[ML]/[MLOH]·[H]	–	9.41(9)	–	–	–

[a]) [9a]. [b]) [14]. [c]) $I = 0.20$M in $NaNO_3$ [12b]. [d]) $I = 0.20$M in $NaNO_3$ [12a].

the N-donors of **6** are involved in the coordination to these metal ions [14], suggesting that the third N-atom of **1** or **2**, and probably also one carboxylate group, are not involved in the coordination to the alkaline earth metal ions, or that the interaction with them is very weak. This is surprising because we expected a full participation of the donor atoms of **1** and, consequently, higher stability constants. Indeed, the coordination of all the donors was predicted for the corresponding complexes of **4** (H_2L^4) [9]. Although X-ray structures of complexes of *N*-acetic acid derivatives of 15-membered macrocycles are scarce [5][18][19] (none of them involving alkaline earth metals or the ligands in study), they show that the size of the cavity is appropriate for metal ions such as Na^+ [18] or Cd^{2+} [19], but also for smaller ions like Cu^{2+} [5]. In all these examples, the full participation of the donors was found. However, **1** and **2** have more amine and carboxylate groups than the ligands for which X-ray structures are available, and as alkaline earth metal ions prefer O- to N-donors, the metal ions will be forced to stay at longer distances from one of the N-atoms, or even not to coordinate to it, in order to achieve better interactions with the other donor atoms.

One additional methylene group in the skeleton of the macrocycle of **1** to form **2** leads to a decrease in the stability constants of the alkaline earth metal complexes, the decrease being more pronounced for larger metal ions (Mg^{2+} is not considered due to the exceptional behavior of its complexes). This effect has already been observed with the complexes of tetraaza- [13], oxatriaza- [15b], or dioxadiazamacrocycles [15a] and of linear ligands, such as H_4edta and H_4tmdta ((propane-1,3-diyldinitrilo)tetraacetic acid) [20][21]. This means that the affinity for the larger metal ions decreases with the cavity size of the macrocycle, contrary to the interpretation based on the size-match selectivity for macrocycles. This apparent paradox was explained by *Hancock* and co-workers [20][21] who found, based on molecular-mechanics calculations, that the lowest strain energy is observed in the case of the 5-membered chelate ring for metal ions with a M–N bond length of 2.50 Å and a N–M–N bond angle of 60°, while the values for the 6-membered chelate ring are 1.6 Å and 109.5°, respectively [20]. Our case is another example of the dependence of the stability constants of complexes on the chelate ring size.

Table 3. *Stability Constants* (log units) *for Metal Complexes of the Ligands with Several Divalent Metal Ions.* $T = 25.0°$; $I = 0.10$M in $(Me_4N)NO_3$.

	Equilibrium quotient	**1** (H_3L^1)	**2** (H_3L^2)	**3** (H_3L^3)[a]	**4** (H_2L^4)[b]	**6** (H_3L^6)[c]
Mn^{2+}	$[ML]/[M]\cdot[L]$	14.44(4)	9.47(3)	–	12.11	16.09
	$[MHL]/[ML]\cdot[H]$	3.98(3)	–	–	–	4.14
	$[M_2L]/[ML]\cdot[M]$	–	3.07(4)	–	–	–
	$[ML]/[MLOH]\cdot[H]$	pp	–	–	–	–
Co^{2+}	$[ML]/[M]\cdot[L]$	16.47(3)	12.31(3)	16.38	13.72	19.54
	$[MHL]/[ML]\cdot[H]$	3.99(2)	5.66(3)	3.73	–	2.64
	$[MH_2L]/[MHL]\cdot[H]$	–	3.44(4)	–	–	–
	$[M_2L]/[ML]\cdot[M]$	3.30(4)	3.71(4)	1.73	2.65	–
	$[M_2HL]/[M_2L]\cdot[H]$	3.95(5)	4.67(5)	–	–	–
	$[ML]/[MLOH]\cdot[H]$	(8.9)	10.49(5)	11.20	–	–
	$[M_2L]/[M_2L(OH)]\cdot[H]$	–	7.11(5)	–	–	–
	$[M_2L]/[M_2L(OH)_2]\cdot[H]^2$	–	15.61(5)	–	–	–
Ni^{2+}	$[ML]/[M]\cdot[L]$	15.52(5)	14.88(2)	14.94	12.37	18.04
	$[MHL]/[ML]\cdot[H]$	4.38(2)	5.07(5)	4.78	–	3.66
	$[M_2L]/[ML]\cdot[M]$	3.59(4)	4.33(3)	1.35	1.9	–
	$[M_2HL]/[M_2L]\cdot[H]$	4.03(5)	4.58(4)	–	–	–
	$[ML]/[MLOH]\cdot[H]$	8.86(3)	(8.6)	11.01	–	–
	$[M_2L]/[M_2L(OH)]\cdot[H]$	–	6.08(7)	–	–	–
	$[M_2L]/[M_2L(OH)_2]\cdot[H]^2$	16.21(7)	13.89(7)	–	–	–
Cu^{2+}	$[ML]/[M]\cdot[L]$	17.25(4)	16.41(4)	17.54	17.79	20.17
	$[MHL]/[ML]\cdot[H]$	3.63(4)	4.76(5)	5.63	–	3.10
	$[MH_2L]/[MHL]\cdot[H]$	–	–	1.49	–	–
	$[M_2L]/[ML]\cdot[M]$	2.96(5)	4.80(3)	–	5.00	–
	$[ML]/[MLOH]\cdot[H]$	(9.5)	(9.8)	11.91	–	–
	$[M_2L]/[M_2L(OH)]\cdot[H]$	(5.7)	5.33(5)	–	–	–
	$[M_2L]/[M_2L(OH)_2]\cdot[H]^2$	12.26(5)	11.93(5)	–	–	–
Zn^{2+}	$[ML]/[M]\cdot[L]$	16.82(2)	12.71(3)	16.38	14.44	18.66
	$[MHL]/[ML]\cdot[H]$	3.69(1)	5.49(2)	3.73	–	2.85
	$[MH_2L]/[MHL]\cdot[H]$	2.05(4)	–	–	–	–
	$[M_2L]/[ML]\cdot[M]$	2.76(5)	3.57(5)	2.14	2.91	–
	$[M_2HL]/[M_2L]\cdot[H]$	3.86(3)	4.79(4)	–	–	
	$[ML]/[MLOH]\cdot[H]$	(9.0)	–	10.68	–	
	$[M_2L]/[M_2L(OH)]\cdot[H]$	7.65(8)	6.11(5)	–	–	
Cd^{2+}	$[ML]/[M]\cdot[L]$	17.83(3)	14.78(2)	16.97	13.43	19.25
	$[MHL]/[ML]\cdot[H]$	3.60(4)	3.76(1)	3.56	–	–
	$[MH_2K]/[MHL]\cdot[H]$	2.0(1)	–	–	–	–
	$[M_2L]/[ML]\cdot[M]$	–	2.55(4)	2.06	2.19	–
	$[ML]/[MLOH]\cdot[H]$	(9.0)	–	10.95	–	–
Pb^{2+}	$[ML]/[M]\cdot[L]$	16.92(2)	13.67(3)	16.58	13.26	19.27
	$[MHL]/[ML]\cdot[H]$	3.62(2)	6.15(2)	4.88	–	3.48
	$[MH_2L]/[MHL]\cdot[H]$	2.0(1)	–	2.18	–	–
	$[M_2L]/[ML]\cdot[M]$	3.48(4)	3.57(4)	3.24	2.44	–
	$[M_2HL]/[M_2L]\cdot[H]$	3.21(4)	5.72(5)	–	–	–
	$[M_2L]/[M_2L(OH)]\cdot[H]$	7.19(7)	6.88(7)	–	–	–
	$[M_2L]/[M_2L(OH)_2]\cdot[H]^2$	14.49(5)	–	–	–	–

[a]) $I = 0.10$M in KCl [11]. [b]) [9a]. [c]) [14].

2.4. *Complexes of the Transition-Metal Ions.* The values of *Table 3* show that the 15-membered ligands **1**, **3**, and **4** have less tendency to form dinuclear species than the 16-membered **2**, and that higher values of K_{M_2L} were found for the Cu^{2+} and Ni^{2+} complexes of **2**. The first-row transition-metal ions usually adopt the coordination numbers four to six. Seven-coordinate complexes for the metal ions of this row are relatively rare [22]. Therefore, they more easily form dinuclear complexes with the ligands studied than the alkaline earth metal ions, and the tendency to form these species increases with the size of the macrocycle, for the same number of donors.

The pM values calculated at neutral pH [23] (see *Table 4*), taking into account the differences in the overall basicity of the ligands shown in *Table 3*, are similar for **1** and **3**, while those for **4** are much lower than for **1** (differences of 2 to 3 units), except in the case of Cu^{2+} and, finally, those for **6** are only one unity higher than for **1**.

Table 4. *pM*[a]) *Values for First-Row Transition-Metal Ions, Cd^{2+}, and Pb^{2+} Complexes of* **1**, **2**, *and Some Other Similar Ligands.* At pH 7.0

	1 (H_3L^1)	**2** (H_3L^2)	**3** (H_3L^3)	**4** (H_2L^4)	**6** (H_3L^6)
pMn	10.44	5.73	–	8.49	10.70
pCo	12.48	8.42	11.90	10.10	14.15
pNi	11.53	10.98	10.50	8.75	12.65
pCu	13.25	12.50	13.08	14.17	14.17
pZn	12.83	8.81	11.90	10.82	13.27
pCd	13.84	10.87	12.49	9.81	13.86
pPb	13.04	9.81	12.11	9.64	13.88

[a]) Values calculated for 100% excess of free ligand at pH 7.0; $C_M = 1.0 \cdot 10^{-5}$ M, $C_L = 2.0 \cdot 10^{-5}$ M, by the *Hyss* program [23]. [b]) Calculated from the published stability constants: **3**, $I = 0.10$M in KCl [11]; **4** [9a]; **6** [14].

Therefore, the values of the stability constants of the mononuclear complexes of **1** with the first-row transition-metal ions are sufficiently high to assume that the three N-atoms of the ligand coordinate to the metals, although it is not possible to ascertain the number of coordinated O-atoms; for most of them, two or three will be free. This behavior is quite different from that of the alkaline earth metal complexes.

The values of log K_{ML} for **1** (H_3L^1) along the first-row divalent transition-metal ions, and also for Cd^{2+} and Pb^{2+}, do not show significant variations (16 – 17 log units for all of them, except for Mn^{2+} for which the stability constant is slightly lower). This means that they do not obey the known *Irving-Williams* order of stability. In contrast, the complexes of **2** (H_3L^2) along this series show a more selective behavior, the Mn^{2+} complex presenting a very low stability constant, and the Cu^{2+} or Ni^{2+} complex showing values of the order of the corresponding complexes for the 15-membered ligand. Additionally, they obey the *Irving-Williams* order of stability.

The lower values of the stability constants of the mononuclear complexes ML of **2** in comparison with those of **1** are in agreement with the behavior already described for the alkaline earth metal complexes. However, the dinuclear species present higher values for the 16-membered ligand **2** than for **1**, in particular for the Ni^{2+} and Cu^{2+} complexes, in agreement with the increase of the size of the cavity. While the formation of the ML complexes implies an arrangement of the donor atoms of the ligand with the

pendant arms directed to the center of the macrocycle, the formation of the dimer, in contrast, requires the reorganization of the donors around two metal centers, far away from each other to minimize repulsions, and so projecting the pendant arms to outside the cavity of the macrocycle. Thus, the more flexible 16-membered ligand **2** loses more configurational energy to organize the donor atoms around one metal ion, as indicated by the lower ML stability constants, and tends to accommodate better two metal ions to form dimers.

2.5. *X-Ray-Diffraction Analysis of [Cu(HL^1)] · 0.5 H_2O.* The coordination geometry of the monoprotonated complex [Cu(HL^1)] · 0.5 H_2O formed from Cu^{2+} and **1** can be described as a distorted compressed trigonal bipyramid (see *Fig. 1*). In *Table 5*, selected bond lengths and angles are shown. The equatorial plane is defined by the atoms N(1), O(1), and N(3), and the axial positions are occupied by N(2) and O(3), O(1) being an O-atom of the macrocyclic backbone and O(3) an O-atom of the carboxylate group bound to N(1) (see *Fig. 1*). The Cu-atom is 0.031(2) Å out of the equatorial plane. The axial angle O(3)–Cu–N(2) is 171.2(1)°, very close to the expected value of 180°. The macrocycle is folded along the direction N(1)···N(3), and this induces not only a long Cu–O(1) equatorial distance (2.408(3) Å) very different from the Cu–N ones (2.066(3) and 2.085(3) Å), but also very short axial distances, *i.e.*, Cu–O(3) 1.906(3) and Cu–N(2) 2.036(3) Å. The strong distortion of the equatorial coordination geometry is also reflected in the values of the equatorial angles very different from the expected 120°, 151.9(1)° for N(1)–Cu–N(3), 132.5(1)° for O(1)–Cu–N(1), and 75.5(1)° for O(1)–Cu–N(3). The dihedral angle between the two planes defined by the seven-membered N(1)···N(3) and the ten-membered N(3)···N(1) chains of the macrocycle is 102.4(4)°. The complex is protonated, and the H-atom has been located in the difference-*Fourier* map near atom O(6) and refined without restrictions. The presence of a disordered H_2O molecule in the crystal structure prevents a complete H-bonding analysis. The shortest H-bonding interaction is between O(7) and H(60), from a symmetry related $(x+1, y, z)$ molecule: O(6)···O(7) = 2.47(4) Å and O(6)–H··· O(7) of 168.8(3)°. This intermolecular interaction could also be responsible for the special position of the carboxylate atom O(7) approaching the coordination sphere of the metal atom.

Five-coordinate copper(II) complexes involving macrocycles which exhibit compressed trigonal-bipyramidal geometries are rare. The parent ligand [15]aneN_3O_2 forms a very peculiar trinuclear complex that contains a μ_3-CO_3 bridging the three metal ions through the O-atoms, [Zn_2Cu([15]aneN_3O_2)$_3$(μ_3-CO_3)], in which each metal ion exhibits a distorted trigonal-bipyramidal geomety, but not a compressed one. The equatorial plane is formed by two N-atoms of the macrocycle and the O-atom of the carbonate, the axial positions are occupied by the third N-atom and one of the O-atoms of the macrocycle. The second O-atom of the macrocycle is not coordinated. The macrocycle is in a folded conformation, although along a different direction [24]. In a similar copper(II) complex, [Cu_3([15]aneN_3O_2)$_3$(μ_3-CO_3)], each Cu-atom adopts a distorted square-pyramidal geometry, with the three N-atoms of the macrocycle and the O-atom of the carbonate forming the basal plane and an O-atom of the ring weakly bound in apical position (2.531(13) Å). In this latter complex, the macrocycle is folded along a direction coincident with that in [Cu(HL^1)], with an identical angle of 103.6(5)° [24].

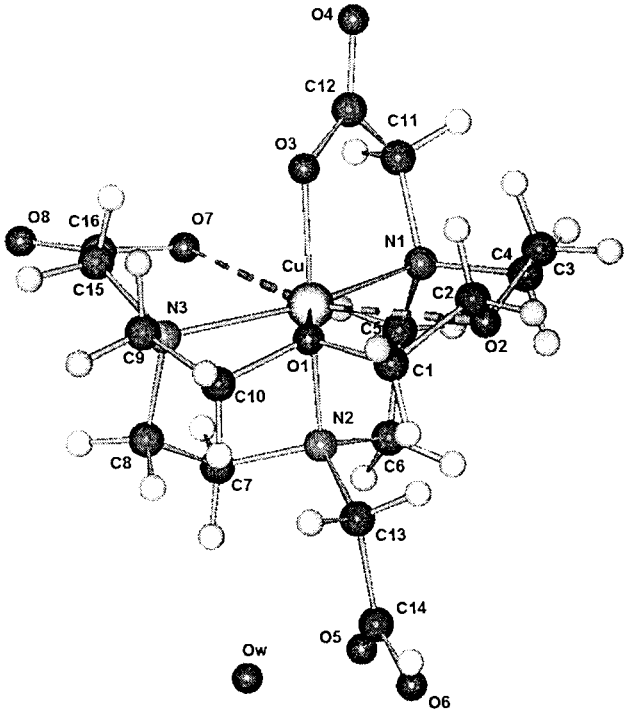

Fig. 1. *Molecular structure of the complex [Cu(HL^1)]·0.5 H_2O formed from Cu^{2+} and* **1** *showing the trigonal-bipyramidal symmetry around Cu^{2+}, with the labelling scheme adopted*. Dashed lines indicate the additional Cu···O longer interactions which lead to the pentagonal-bipyramidal geometry.

Table 5. *Selected Bond Lengths* [Å] *and Angles* [deg] *of [Cu(HL^1)]·0.5 H_2O*

Cu–O(3)	1.906(3)	Cu–N(2)	2.036(3)	Cu–O(2)	2.727(4)[a])
Cu–O(1)	2.408(3)	Cu–N(3)	2.085(3)	Cu–O(7)	2.932(4)[a])
Cu–N(1)	2.066(3)				
O(3)–Cu–N(1)	85.8(1)	O(3)–Cu–N(2)	171.2(1)	O(3)–Cu–N(3)	95.5(5)
O(1)–Cu–N(1)	132.5(1)	O(1)–Cu–O(3)	86.1(1)	O(1)–Cu–N(2)	102.7(1)
N(2)–Cu–N(3)	87.9(1)	N(1)–Cu–N(3)	151.9(1)	N(2)–Cu–N(1)	87.3(1)
O(1)–Cu–N(3)	75.5(1)	O(2)–Cu–O(7)	154.5(2)[a])	O(2)–Cu–O(1)	61.4(2)[a])
O(2)–Cu–N(1)	71.8(2)[a])	O(2)–Cu–N(2)	93.3(1)[a])	O(2)–Cu–N(3)	136.1(2)[a])
O(7)–Cu–N(2)	88.9(2)[a])	O(7)–Cu–N(3)	69.4(2)[a])	O(7)–Cu–N(1)	82.9(2)[a])

[a]) Bond lengths and angles based on heptacoordination.

The analysis of the above structures suggests that the size of the cavity of the macrocycle [15]aneN_3O_2 is too large to accommodate Cu^{2+} in a five-coordinate symmetry, as the macrocycle needs to fold and one of the O-atoms remains uncoordinated. To complete the coordination sphere, the Cu-atom accepts a donor from a pendant arm, such as in [Cu(HL^1)]·0.5 H_2O, or from another ligand, such as the carbonate in the cases described by *Paoletti* and co-workers [24]. It is interesting that in the structure of our complex, the second O-atom of the macrocycle, O(2), and the atom

O(7) of the carboxylate arm bound to N(3), are not unambiguously involved in the coordination to the Cu-atom in the distorted compressed trigonal-bipyramid arrangement described before. Actually they are coplanar with atoms N(1), O(1), and N(3) of the trigonal bipyramid defining the equatorial plane (O(1)–O(2)–N(1)–O(7)–N(3)) of a compressed pentagonal bipyramid, where the apical positions are still occupied by O(3) and N(2). Although the distances Cu–O(2) and Cu–O(7) are too long to be considered covalent bonds to Cu^{2+} (2.727(4) and 2.932(4) Å, resp.), those atoms are in the appropriate pentagonal positions. The atoms O(7) and O(2) almost bisect the angles N(3)–Cu–N(1) and N(1)–Cu–O(1) of the trigonal-bipyramidal geometry, generating a rather 'non-distorted' equatorial pentagon, where the angles are not far from the expected 75°: N(1)–Cu–O(2) 71.8(2)°, O(2)–Cu–O(1) 61.4(2)°, O(1)–Cu–N(3) 75.5(1)°, N(3)–Cu–O(7) 69.4(2)°, and O(7)–Cu–N(1) 82.9(2)°. Also to allow O(7) to occupy such a position, it is necessary that the carboxylate group to which it belongs twists towards the Cu-atom instead of swaying out, as expected for a free carboxylate group. The equatorial plane thus defined by atoms O(1), O(2), N(1), O(7), and N(3) (maximum deviations are for N(3) and O(1), *i.e.* 0.213(2) and 0.191(3) Å, resp.) is almost perpendicular to the plane containing O(3), Cu, and N(2). The Cu-atom is 0.081(5) Å out of this equatorial plane. This geometry is clearly seen from *Fig. 1*. In this arrangement, only the atom O(6) of the carboxylate bound to N(2) stays out of the coordination sphere, which is understandable as it is protonated.

Curiously, the seven-coordinate compressed pentagonal bipyramid is the geometry adopted by the Cu^{2+} complexes of other 15-membered macrocycles, such as **4** (H_2L^4) in $[CuL^4]\cdot 2H_2O$ [5][6], [15]crown-5 (1,4,7,10,13-pentaoxacyclopentadecane) in $[Cu([15]crown\text{-}5)(H_2O)_2]^{2+}$ [7], or B[15]crown-5 (2,3-benzo-1,4,7,10,13-pentaoxacyclopentadec-2-ene) in $[Cu(B[15]crown\text{-}5)(H_2O)_2]^{2+}$ [7] and $[Cu(B[15]crown\text{-}5)Cl_2]\cdot CHCl_3$ [8]. In contrast to our case, where the macrocycle is folded along the N(1)···N(3) direction, with the pendant carboxylate arms coordinating in a *cis*-arrangement, in all known seven-coordinate Cu^{2+} complexes, the metal ion adopts a D_{5h} symmetry. In these last cases, the Cu-atom is located inside the cavity of the macrocycle, or is slightly displaced from the basal plane, with the five donor atoms of the macrocycle forming the pentagonal plane, and all the Cu-(donor atom) distances having covalent bond distances (between 1.910 and 2.518 Å). In $[CuL^4]\cdot 2H_2O$ [5][6], the O-atoms of the *N*-carboxylate substituents occupy the axial positions at shorter distances (1.945(6) and 1.925(6) Å) in a *trans*-arrangement of the pendant arms, while the equatorial Cu–O distances range from 2.093 to 2.518 Å. In $[Cu(B[15]crown\text{-}5)Cl_2]$ [8], the axial Cu–Cl distances (2.254(2) and 2.242(2) Å) are shorter and closer to the equatorial ones (2.240 to 2.337 Å). In $[Cu([15]crown\text{-}5)(H_2O)_2]^{2+}$ or $[Cu(B[15]crown\text{-}5)(H_2O)_2]^{2+}$ [7], the apical distances to the O-atom of H_2O molecules (1.910(5) Å for the former and 1.922(6) and 1.913(5) Å for the latter complex) are again much shorter than the equatorial ones (2.133(5) to 2.313(4) Å for the former and 2.150(6) to 2.314(5) Å for the latter complex).

Why does the complex $[Cu(HL^1)]$ adopt a structure with the macrocycle in a folded arrangement, and not a planar one such as that exhibited by $[Cu(L^4)]$ [5][6], since in both cases, 15-membered macrocycles with *N*-acetic-acid arms are involved? In our case, Cu^{2+} prefers to coordinate the three available N-atoms of the ring and as many O-atoms located at coordination distances as needed to satisfy its coordination

number. The preference for N-atoms is usual for this metal ion, but implies a folded arrangement of the macrocycle. The differences between the crystal structures of our complex and those involving crown ethers [7][8] are more understandable, because the appending of flexible arms that also contain donor atoms may induce different structures.

2.6. *Structural Studies in Solution.* Spectroscopic UV/VIS/near-IR data for Co^{2+}, Ni^{2+}, and Cu^{2+} complexes of **1** (H_3L^1) and **2** (H_3L^2) and EPR parameters for the Co^{2+} and Cu^{2+} complexes of both ligands in aqueous solution are collected in *Tables 6* and *7*, respectively.

Cobalt(II) Complexes. The electronic spectra of $[CoL^1]^-$ and $[CoL^2]^-$ are similar, both exhibiting a multiple-structured band in the VIS region with shoulders at higher and lower energies and a large near-IR band, all the bands having very low intensities (*Table 6*). These spectra point to six-coordinate environments of high-spin species [25][26]. The calculated values of the octahedral field-splitting parameter ($10Dq$) [26] of 11422 cm^{-1} for $[CoL^1]^-$ and 10392 cm^{-1} for $[CoL^2]^-$ show the stronger crystal-field stabilization energy (CFSE) of the former complex, in agreement with the determined stability-constant values. On exposure to air, both complexes undergo a very slow degradation with time at pH 7.5 – 8.0.

The EPR spectra of the two Co^{2+} complexes at 4 – 10 K show as principal feature a broad and intense band at low field, centered at *ca.* 1200 G, and anisotropic g values. The apparent g values for $[CoL^1]^-$ are $g_1' = 5.49$, $g_2' = 4.50$, and $g_3' = 2.0$, and no hyperfine splitting is detected. The $[CoL^2]^-$ complex at pH 5.88 (in parentheses the values obtained in glycerol/H_2O 1:1) exhibits a very peculiar spectrum with signals corresponding to two species, the first one with resonances at 8.07, 1.5, and *ca.* 1 (8.31, 1.5, and *ca.* 1) with resolved hyperfine structure in the low-field resonance due to the interaction with the Co^{2+} nucleus ($I = 7/2$) and hyperfine constant $A = 422.9 \cdot 10^{-4}$ cm^{-1} ($443.7 \cdot 10^{-4}$ cm^{-1}); the other species presents resonances very similar to those found for $[CoL^1]^-$ ($g_1' = 5.58$, $g_2' = 4.43$, and $g_3' = 2.0$ ($g_1' = 5.14$, $g_2' = 4.36$, and $g_3' = 2.0$)), without resolved hyperfine splitting (see *Fig. 2*). The line at $g \approx 2.0$ is contaminated

Table 6. *UV/VIS/Near-IR Data for the Co^{2+}, Ni^{2+}, and Cu^{2+} Complexes of* **1** (H_3L^1) *and* **2** (H_3L^2). $T = 25.0°$.

Color	pH	UV/VIS/near-IR (λ_{max}/nm (ε_{molar}/M^{-1} cm^{-1}))
$[CoL^1]^-$ pink	7.32	1159 (6.7), 985 (7.6), 628 (sh, 9.6), 564 (sh, 12.5), 463 (sh., 15.3), 348 (sh, 29.2)
$[NiL^1]^-$ green	7.14	1158 (sh, 20.8), 1100 (20.1), 1001 (sh, 13.0), 916 (sh, 11.1), 802 (3.8), 668 (sh, 4.5), 632 (5.6), 616 (sh, 5.3), 355 (27.2), 301 (99.6)
	3.33	1175 (sh, 12.3), 1100 (sh, 12.1), 1001 (13.2), 875 (sh, 9.8), 760 (5.5), 682 (sh, 6.2), 626 (7.2), 612 (7.3), 355 (sh, 26.6), 299 (sh, 88.6)
$[CuL^1]^-$ blue	7.05	1158 (4.1), 990 (sh, 10.2), 828 (sh, 46.7), 662 (121.4), 620 (sh, 106.5), 292 ($2.76 \cdot 10^3$)
$[CoL^2]^-$ pink	7.50	1148 (sh, 7.7), 1095 (6.6), 1010 (sh, 6.2), 638 (sh, 14.5), 562 (sh, 18.3), 524 (sh, 19.7), 486 (sh, 23.3), 456 (sh, 23.7), 294 (sh, 80.8)
$[NiL^2]^-$ green	7.43	1161 (sh, 16,3), 1085 (16.3), 965 (sh, 12.1), 686 (sh, 11.8), 628 (16.0), 612 (16.1), 356 (sh, 45.1)
	3.58	1151 (sh, 9.5), 1085 (sh, 10.6), 965 (12.2), 823 (sh, 7.1), 765 (6.5), 666 (sh, 7.9), 628 (sh, 8.1), 594 (9.8), 349 (sh, 31.6)
$[CuL^2]^-$ blue	7.99	1169 (6.2), 908 (sh, 23.2), 831 (sh, 36.0), 750 (sh, 65.3), 638 (98.2), 625 (sh, 96.2), 290 ($3.5 \cdot 10^3$)

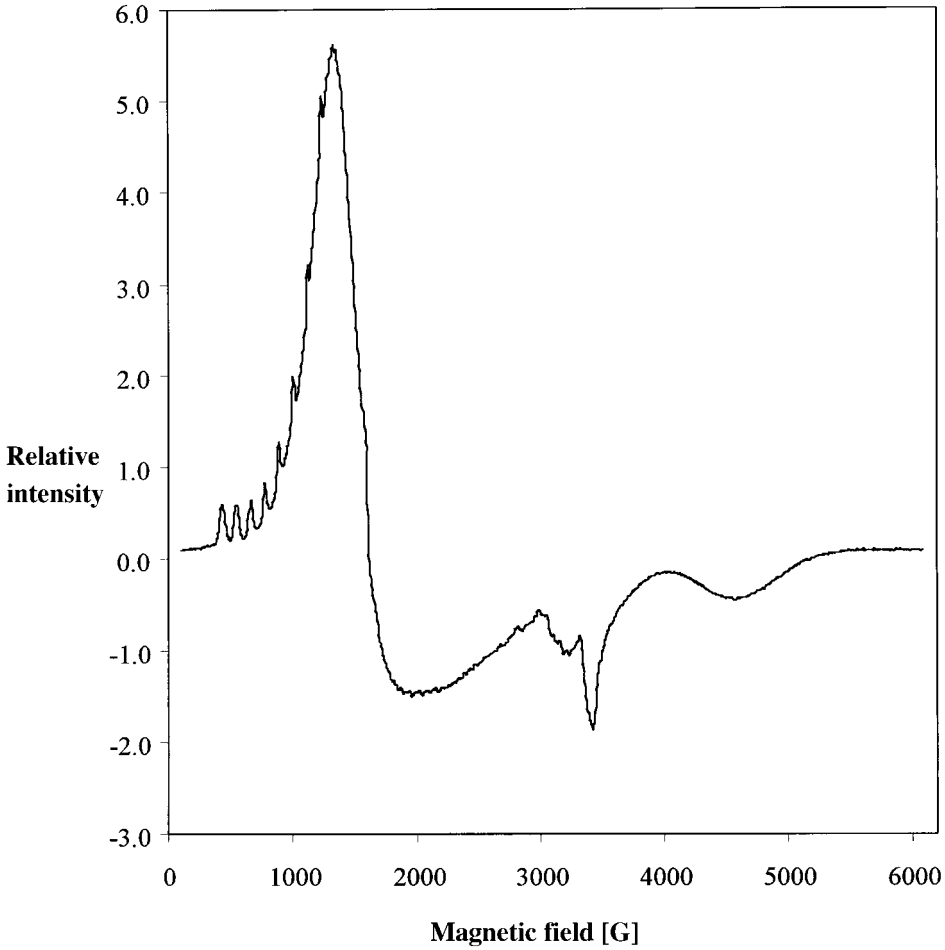

Fig. 2. *EPR X-Band spectrum of the* Co^{2+} *complex of* **2** (H_3L^2). Recorded in glycerol/H_2O 1:1 at 10 K, microwave power 2.4 mW, modulation amplitude 0.9 mT, and frequency (ν) 9.641 GHz.

with a small amount of the typical signal of the Co^{2+} complex with O_2 [27]. The spectra are typical of high-spin Co^{2+} complexes ($S = 3/2$) in a rhombically distorted environment and can be interpreted in terms of a $S = 1/2$ effective spin Hamiltonian [28][29].

Compilation of experimental data has shown that spectra of octahedral and square-pyramidal complexes show at least one large Co hyperfine structure resolved [28][29]. Consequently, $[CoL^1]^-$ and $[CoL^2]^-$ have one of these symmetries. The low intensity exhibited by their electronic spectra and the absence of a weak band appearing in the 830–660 nm region suggest that our Co^{2+} complexes adopt distorted octahedral geometries. Very few complexes present g_1 values of the order of 8 as for $[CoL^2]^-$ [30][31], but values similar to that of $[CoL^1]^-$ are common [29] and found in some enzymes, such as alkaline phosphatase of *E. coli* [32].

Nickel(II) Complexes. The electronic spectra observed for the green solutions of both Ni^{2+} complexes, $[NiL^1]^-$ and $[NiL^2]^-$, are characteristic of a tetragonal (D_{4h}) symmetry (*cf. Table 6*) [26][33–35]. The band in the VIS region of both complexes appears as a well-defined doublet, and the ratio of the near-IR band (ν_1) and of that appearing in the visible (ν_2) is 1.74 for $[NiL^1]^-$ and 1.73 for $[NiL^2]^-$, also characteristic of tetragonal Ni^{2+} [34]. The bands of our spectra are tentatively assigned, according to the considerations of *Busch* and co-workers [35] for some tetraazamacrocycles, and values of Dq^{xy} and Dq^z were calculated based on these assignments ($Dq^{xy} = 1582\ cm^{-1}$ and $Dq^z = 236\ cm^{-1}$ for $[NiL^1]^-$, and $Dq^{xy} = 1592\ cm^{-1}$ and $Dq^z = 251\ cm^{-1}$ for $[NiL^2]^-$). These field-splitting parameters are identical for both complexes, in agreement with the stability-constant results (*Table 3*).

Copper(II) Complexes. The EPR spectra of the two Cu^{2+} complexes at the Cu^{2+}/ligand ratio 1:1 are shown in *Fig. 3* at two pH values for each complex. The spectra at the lower pH show the presence of two and three species, respectively, as can be easily seen by the splitting of the bands at low field (*Fig. 3*, *a* and *c*) but at pH *ca.* 6.7, only one species is present, and the spectra of the complexes with **1** and **2** are very similar. The simulation of the spectra [36] indicate three different principal *g* values, showing that the Cu^{2+} ion in these complexes is in a rhombically distorted ligand field. The hyperfine coupling constants and *g* values are compiled in *Table 7*, together with those of other known complexes. The complexes with **1** and **2** show rhombic symmetry with elongation of the axial bonds and a $d_{x^2-y^2}$ ground state. Trigonal-bipyramidal or tetragonal geometries involving compression of axial bonds must be excluded [7][22].

The EPR parameters and the maximum of the d-d absorption band of $[CuL^1]$ are between those of the complexes $[Cu(L^7)(H_2O)]^{2+}$ [37] and $[CuL^8]$ [38], but closer to the latter. The crystal structure of $[Cu(L^7)(H_2O)]^{2+}$ shows that the Cu^{2+} adopts a distorted square-pyramidal geometry, with the basal plane formed by the donor atoms of the macrocycle and a H_2O molecule in axial position [37], while $[CuL^8]$ adopts the geometry of a distorted octahedron, tetragonally elongated, where the equatorial plane is formed by the three N-atoms of the macrocycle and the O-atom of one carboxylate group, and where the axial positions are occupied by the O-atom of the other carboxylate group and the O-atom of the ring [38]. The EPR parameters of both complexes (*Table 7*) are in agreement with the X-ray crystal structures [39–41] and, therefore, those of $[CuL^1]^-$ indicate a six-coordinate symmetry, with the equatorial field slightly stronger than that of $[CuL^8]$, having three N- and one O-atoms in the equatorial plane and two O-atoms in axial positions. The $[CuL^2]^-$ ion exhibits EPR and electronic spectra very similar to those of $[CuL^1]^-$, but showing a slightly higher A_z value, and its d-d absorption band is shifted to higher energies, which may suggest a more distorted environment for the Cu-atom in this complex.

At pH 3.18, the speciation diagram for Cu^{2+}/**1** (H_3L^1) in aqueous solution at room temperature reveals the presence of 68% of $[Cu(HL^1)]$, 5% of aqueous Cu^{2+} ion, 25% of $[CuL^1]^-$, and 2% of $[Cu_2L^1]^+$ (*Fig. 4*). The EPR spectrum shows only two species, one exhibiting $g_\perp = 2.075$, $g_\parallel = 2.331$, and $A_\parallel = 142.6 \cdot 10^{-4}\ cm^{-1}$, which corresponds to $[Cu(H_2O)_6]^{2+}$ [42], and the other one ($g_1 = 2.063$, $g_2 = 2.085$, $g_3 = 2.257$, and $A_3 = 173.1 \cdot 10^{-4}\ cm^{-1}$), corresponding to the protonated complex. The EPR parameters of $[CuL^1]^-$ and the protonated complex $[Cu(HL^1)]$ are so similar (see *Table 7*) that the small amount of the former species indicated by the speciation diagram cannot be

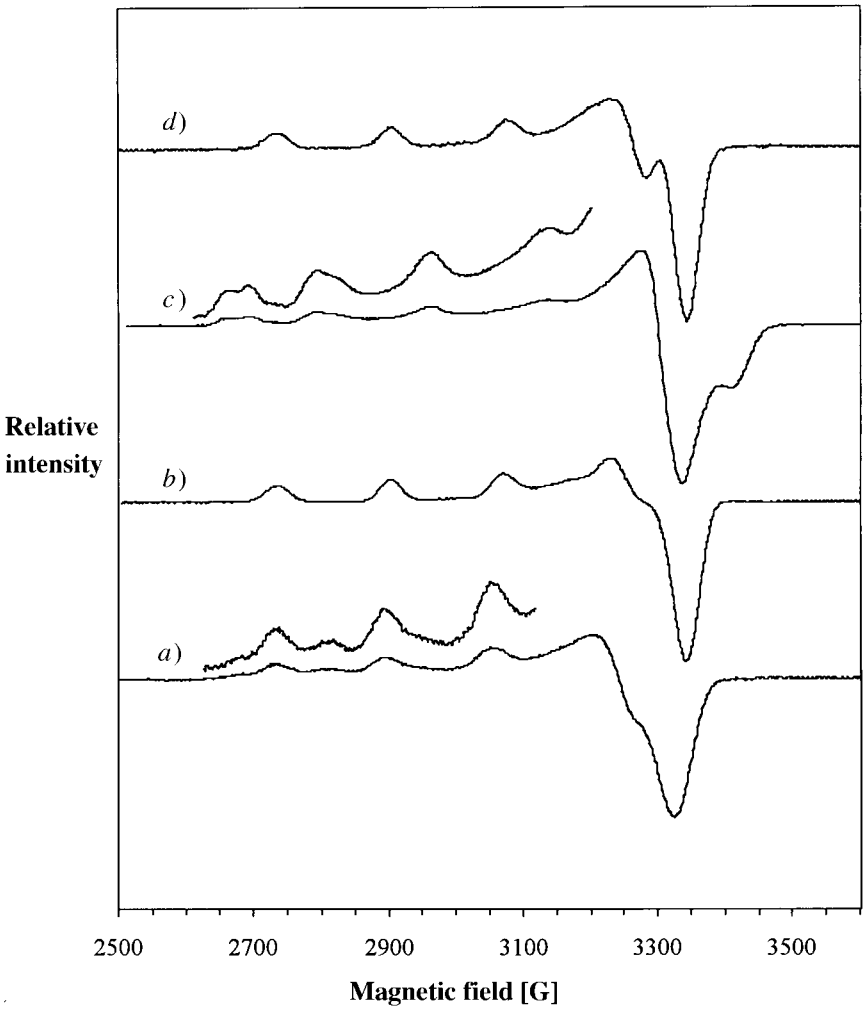

Fig. 3. *EPR X-Band spectra: Cu^{2+} complexes of* **1** (H_3L^1) *in a 1:1 ratio* a) *at pH 3.18 and* b) *at pH 6.67*; *Cu^{2+} complexes of* **2** (H_3L^2) *in a 1:1 ratio* c) *at pH 3.36 and* d) *at pH 6.72*. Recorded in 1.0M $NaClO_4$ at 127 K (*a*) and *c*)) and 107 K (*b*) and *d*)), microwave power 2.4 mW, modulation amplitude 0.9 mT, frequency (*ν*) 9.403, 9.410, 9.402, and 9.618 GHz for *a*), *b*), *c*), and *d*), resp.

distinguished in the spectrum. Therefore, in solution both complexes $[Cu(HL^1)]$ and $[CuL^1]^-$ exhibit similar structures, the former having a slightly weaker equatorial field, in contrast to what was found in the solid state by X-ray diffraction. Indeed, trigonal(or pentagonal)-bipyramidal Cu^{2+} complexes have a $3d_{z^2}$ ground state and exhibit very characteristic EPR spectra with reverse *g*-anisotropy ($g_z < (g_x + g_y)/2$ and g_z values *ca.* 2) [7][22].

In the EPR spectrum of Cu^{2+}/**2** (H_3L^2) recorded at pH 3.36, the presence of three species was observed. One of them is also $[Cu(H_2O)_6]^{2+}$ ($g_\perp = 2.053$, $g_\parallel = 2.400$, and $A_\parallel = 146.8 \cdot 10^{-4}\ cm^{-1}$). The second species, which exists in a small amount, has g_z and

Table 7. *EPR Data for the Copper(II) Complexes of* **1** (H_3L^1) *and* **2** (H_3L^2) *and of Other Similar Complexes*

	λ_{max}/nm (ε_{molar}/M^{-1} cm^{-1})	EPR Parameters (A_i/cm^{-1})						Ref.
		g_x	g_y	g_z	$A_x \cdot 10^4$	$A_y \cdot 10^4$	$A_z \cdot 10^4$	
$[Cu(HL^1)]$	–	2.063	2.085	2.257	14.7	33.0	173.1	[a]
$[CuL^1]^-$	662 (121.4)	2.046	2.078	2.246	12.9	33.5	175.2	[a]
$[CuL^2]^-$	638 (98.2)	2.055	2.071	2.246	6.9	29.4	182.5	[a]
$[CuL^7]^{2+}$	622 (147)	2.050	2.059	2.224	10.9	20.5	183.1	[37]
$[CuL^8]$	686 (95.8)	2.040	2.087	2.262	0.7	18.4	163.0	[38]

[a]) This work.

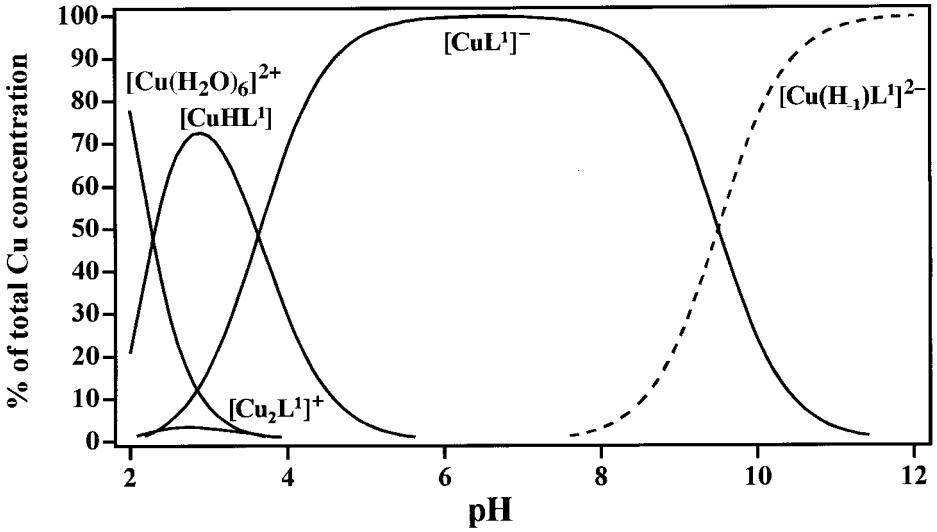

Fig. 4. *Species-distribution curves calculated for an aqueous solution containing* Cu^{2+} *and* **1** (H_3L^1) *at a molar ratio of 1:1.* Percentages relative to the total amount of Cu^{2+} at an initial value of $1.25 \cdot 10^{-3}$ M.

A_z parameters, taken directly from the corresponding signals of the spectrum, similar to those of $[CuL^2]^-$, which can be assigned to $[Cu(HL^2)]$. The third species is a copper(II) dimer (see below). These three species also exist in solution at room temperature, as given by the speciation diagram; however, the protonated species is dominant, while at low temperature it is only residual.

EPR Spectra of solutions of Cu^{2+} with **1** (H_3L^1) and **2** (H_3L^2) in 2:1 ratio, at the pH corresponding to the maximum formation of the dimer $[Cu_2L]^+$, were also recorded (pH *ca.* 4). The spectrum of the former solution reveals that the $[Cu(H_2O)_6]$ complex is the main species, indicating that under these conditions, the excess Cu^{2+} in solution does not form the dimer species but coordinates mainly to H_2O molecules; this is expected if one takes into account the low value of the stability constant determined for this complex (*Table 3*). However, the latter solution, containing **2**, gives the spectrum shown in *Fig. 5*, which is typical of a copper(II) dimer complex, although, at high field, the presence of the monomeric species is clearly perceived. Indeed, in addition to the signal at $g \approx 2$, a weak signal at $g = 4.2$ (1630 G) was observed (see *Fig. 5*). The

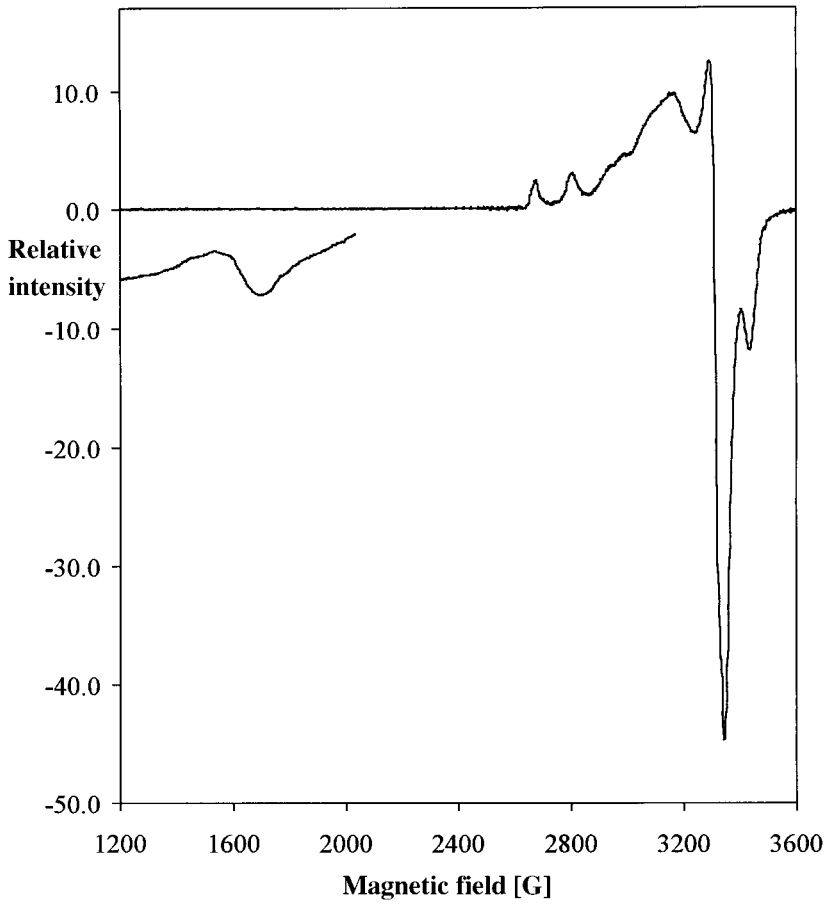

Fig. 5. *EPR X-Band spectra of the* Cu^{2+} *complexes of* **2** (H_3L^2) *in 1.9:1 ratio.* Recorded at pH 4.0 in 1.0M $NaClO_4$ at 130 K. The signal at low field was obtained at 4 K and is amplified in the bottom. Microwave power 2.4 mW, modulation amplitude 0.9 mT, frequency (ν) 9.616, and 9.642 GHz for the $\Delta M_s = 1$ and $\Delta M_s = 2$ transitions, resp.

spectrum was recorded under conditions of maximum concentration of the dimer (at pH *ca.* 4 and Cu^{2+}/**2** 1.9:1), but [$Cu(HL^2)$] is also expected, as shown in *Fig. 6*. Speciation diagrams performed at different metal to ligand ratios show that it is not possible to find experimental conditions where only the $[Cu_2L^2]^+$ species exists. The Cu^{2+}/**2** 1.9:1 ratio is the best compromise. Increasing the amount of the ligand also increases the percentage of the [$Cu(HL^2)$] species, and the increase of the amount of the metal ion increases that of the free metal in solution. The EPR spectrum obtained can be interpreted as that of a coupled binuclear copper site with a $S = 1$ total spin and zero-field splitting, having two types of signals in the $\Delta M_s = 1$ and $\Delta M_s = 2$ regions [43]. The resonance corresponding to the $\Delta M_s = 2$ transition was observed at low temperatures (4 K) as a broad signal, and no hyperfine structure due to the coupling with the two Cu^{2+} nuclei was observed, in spite of the several media tried. This spectrum

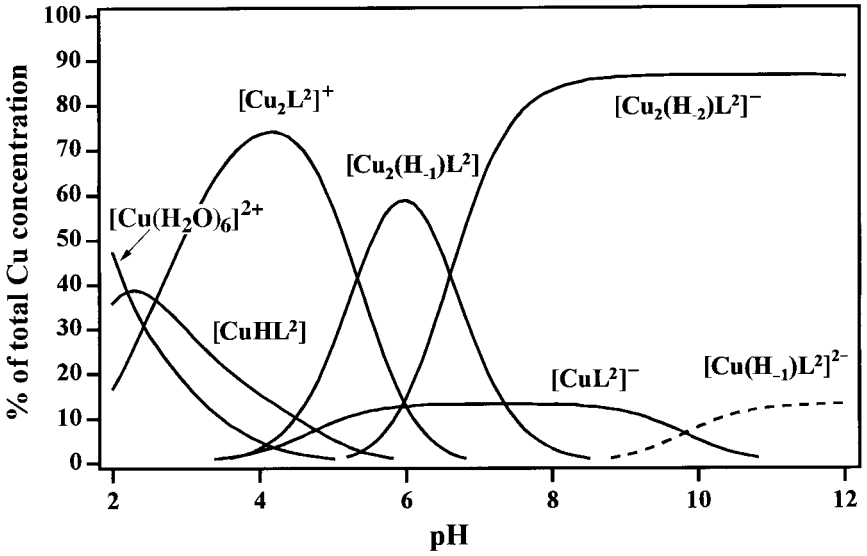

Fig. 6. *Species-distribution curves calculated for an aqueous solution containing* Cu^{2+} *and* **2** (H_3L^2) *at a molar ratio of 1.9:1.* Percentages relative to the total amount of Cu^{2+} at an initial value of $2.50 \cdot 10^{-3}$ M.

indicates a Cu–Cu distance between *ca.* 3 and 5 Å for our dimer [44]. Indeed, for small distances, the zero-field-split components of both transitions overlap, and when the distances are larger, the intensity of the band at low field will be low [44].

3. Conclusions. – The two new 15-membered dioxatriazacyclopentadecanetriacetic acids **1** (H_3L^1) and **2** (H_3L^2) were synthesized. In spite of the size of the macrocycle and the high number of donor atoms, only mononuclear complexes were found for both ligands with the alkaline-earth metal ions. The stability constants of these complexes are lower than expected, possibly due to non-involvement of the third N-atom of the macrocycles in the coordination and, probably, also of one carboxylate group (or only a very weak interaction exists with them). The increase of the framework of the macrocycle **1** (H_3L^1) by only one CH_2 group to form **2** (H_3L^2) leads to an enormous decrease in the thermodynamic stability of the alkaline-earth metal complexes. The ligand **4** (H_2L^4) forms with Cu^{2+} a complex with a compressed pentagonal-bipyramidal arrangement of the donor atoms where the O-atom of the two carboxylate groups occupy the axial positions. Due to the complete encapsulation of the metal ion, this complex has a high stability constant [5][6]. In contrast, the first-row transition divalent metal complexes of $(L^1)^{3-}$ have stability constants lower than would be expected if the metal ions were encapsulated in a similar geometry. Spectral data of the complexes with Co^{2+}, Ni^{2+}, and Cu^{2+} show that they adopt an octahedral geometry in which the three N-atoms of the ring are involved in the coordination. Three O-atoms complete the coordination sphere, one of which probably belongs to the macrocyclic framework, with the other two coming from carboxylate groups. One of the carboxylate arms will be free and protonated at relatively high values of pH, as evidenced by the values of the first protonation constant of the complexes. It was, therefore, possible to

obtain crystals of the monoprotonated form of the copper(II) complex. The structure adopted by $[Cu(HL^1)]\cdot 0.5\,H_2O$ in the crystal, different from that exhibited in solution as shown by EPR spectroscopy, is a compressed distorted trigonal bipyramid with the macrocycle in a folded conformation, with two other atoms in the equatorial plane, but at distances that are a bit too long to be considered coordination distances, halfway toward forming a pentagonal bipyramid. The metal complexes of $(L^2)^{3-}$ have lower and more selective stability constants for the metal ions studied, as would be expected. Due to the larger cavity size of the macrocycle **2** (H_3L^2), the tendency to form dimer complexes increases, as demonstrated by the higher values of the stability constants of these species in solution, and also by the evidence of the presence of these species by EPR spectroscopy.

Experimental Part

Reagents. The parent ligands 1,4-dioxa-7,10,13-triazacyclopentadecane and 1,4-dioxa-7,11,14-triazacyclohexadecane were synthesized as previously reported [10]. All the chemicals were of reagent grade and used as supplied without further purification. The ion-exchange resin (*Dowex 1 × 8*, 20–50 mesh, in the Cl^- form) was treated with 1M formic acid or a 5% KOH soln. before use. ^{1}H- and ^{13}C-NMR: δ in ppm rel. to 3-(trimethylsilyl)(2,2,3,3-D_4)propanoic acid sodium salt and dioxane, resp.

1,4-Dioxa-7,10,13-triazacyclopentadecane-7,10,13-triacetic Acid (**1**; H_3L^1). A conc. soln. of the tris(hydrochloride) of 1,4-dioxa-7,10,13-triazacyclopentadecane (2.48 mmol, 0.80 g) was added to a potassium bromoacetate soln. (obtained by addition of 3M KOH to conc. aq. bromoacetic acid (7.7 mmol, 1.07 g) at 5°), in aq. basic soln. The temp. was increased during the reaction to a maximum of 80°, and the pH was kept between 10 and 12 by slow addition of 3M KOH (6.6 ml) during 72 h. Then the mixture was cooled and the pH adjusted to 2 with 3M HBr. After concentration, MeOH was added and the inorg. matter formed was filtered off. The filtrate was submitted to ion exchange (resin in the formate form; column 28.0 × 2.0 cm; elution with $5\cdot 10^{-3}$M HCOOH, flow rate 1.0 ml min^{-1}, 15-ml fractions). Fractions 17–19 were partly evaporated, and upon addition of MeOH, pure **1** (68%) precipitated. White solid. M.p. 219–221° (dec.); ^{1}H-NMR (D_2O): 3.05 (*t*, 4 H); 3.43–3.48 (*m*, 10 H); 3.63 (*s*, 4 H); 3.77 (*m*, 8 H). ^{13}C-NMR (D_2O): 48.70; 52.15 (*d*); 54.23; 55.86; 63.51; 69.50; 169.40; 174.01. Anal. calc. for $C_{16}H_{29}N_3O_8\cdot H_2O$: C 46.9, H 7.6, N 10.3; found: C 46.8, H 7.7, N 10.0.

1,4-Dioxa-7,10,14-triazacyclohexadecane-7,10,14-triacetic Acid (**2**; H_3L^2). As described for **1**, the tris(hydrochloride) of 1,4-dioxa-7,10,14-triazacyclohexadecane (2.96 mmol; 1.0 g) was condensed with potassium bromoacetate for 96 h. On workup, the filtrate was submitted to ion exchange (resin in the OH^- form, column 28.0 × 2.0 cm), washing with H_2O, elution with 0.1M HBr, 1.0 ml min^{-1}). After concentration and addition of EtOH, pure **2** (69%) precipitated. M.p. 224–226° (dec.). ^{1}H-NMR (D_2O): 2.10 (*q*, 2 H); 3.12 (*t*, 4 H); 3.47–3.59 (*m*, 10 H); 3.69 (*m*, 4 H); 3.84 (*m*, 8 H). ^{13}C-NMR (D_2O): 19.63; 48.82; 49.92; 51.15; 51.93; 53.70; 54.70 (*d*); 55.48; 57.37; 64.46; 64.73; 69.78; 70.12; 168.27; 168.73; 170.58. Anal. calc. for $C_{17}H_{34}Br_3N_3O_8\cdot 2\,H_2O$: C 29.8, H 5.6, N 6.1; found: C 29.9, H 5.6, N 6.1.

Hydrogen [1,4-Dioxa-7,10,13-triazacyclopentadecane-7,10,13-triacetato(4–)-κN^7,κN^{10},κN^{13},κO^7]copper(1–) Hydrate (2:1) ($[Cu(HL^1)]\cdot 0.5\,H_2O$). $Cu(NO_3)_2\cdot 3\,H_2O$ (0.096 mmol, 1 ml) was added to a stirred soln. of **1** (0.041 g, 0.1 mmol) in H_2O (*ca.* 1 ml) and the pH increased to *ca.* 3.5 by addition of KOH. The mixture was kept overnight and then evaporated. The residue was taken in MeOH and the precipitate of inorganic material filtered off. The filtrate was again concentrated, and blue crystals were formed within six days when Et_2O was allowed to diffuse into the soln. at *ca.* 4°: 70% of $[Cu(HL^1)]\cdot 0.5\,H_2O$.

Potentiometric Measurements. All solns. were prepared with demineralized H_2O obtained by a *Millipore/Milli-Q* system. Metal-ion solns. were prepared from the nitrate salts of the metals, and carbonate-free solns. of the titrant, $(Me_4N)OH$ were freshly prepared as described before [17]. The equipment used was described [17]. The temp. was kept at 25.0 ± 0.1° and the ionic strength of the solutions at 0.10M with $(Me_4N)NO_3$.

The $[H^+]$ of the solns. was determined by the measurement of the electromotive force of the cell, $E = E'^0 + Q\log[H^+] + E_j$. E'^0, Q, E_j, and $K_w = [H^+]\cdot OH]$ were obtained as described previously [17]. The term pH is defined as $-\log[H^+]$. The value of K_w was found equal to $10^{-13.80}$ M^2.

The potentiometric equilibrium measurements were made in the absence of metal ions and in the presence of each metal ion for which the C_M/C_L ratios were 1:1 and 2:1, in a minimum of two replicates. The equilibrium

of the metal complexation reactions was sufficiently fast to allow automatic acquisition of data, and the same values of the constants were obtained from either the direct or the back-titration curves.

Protonation constants or stability constants of the various species were calculated by fitting the potentiometric data obtained for the free ligand or for the solns. of different ligand/metal ratios by the SUPERQUAD program [45]. The results were obtained in the form of overall stability constants, $\beta_{M_mH_hL_l}$ values. Mononuclear species [ML], [MH_iL] ($i = 1, 2$), and [$MH_{-1}L$], and also dinuclear species [M_2HL], [M_2L], [$M_2H_{-1}L$], and [$M_2(H_{-1})_2L$], were found for most of the metal ions studied with both ligands (being $\beta_{MH_{-1}L} = \beta_{ML(OH)} \cdot K_W$, $\beta_{M_2H_{-1}L} = \beta_{M_2L(OH)} \cdot K_W$, and $\beta_{M_2(H_{-1})_2L} = \beta_{M_2L(OH)_2} \cdot (K_W)^2$). Differences (in log units) between the values of protonated or hydrolyzed and non-protonated constants, resp., for the mono- and dinuclear reactions, provide the stepwise reaction constants. The errors quoted are the standard deviation of the overall stability constants given directly by the program for the input data, which include all the experimental points of all titration curves. The standard deviations of the stepwise constants, shown in *Tables 1–3*, were determined by the normal propagation rules.

Spectroscopic Studies. Electronic spectra were measured with a *Shimadzu* model *UV-3100* spectrophotometer for UV/VIS/near-IR, with aq. solns. of the complexes prepared by adding of the metal ion (as nitrate salt) to the ligand at the appropriate pH value. EPR-Spectroscopic measurements of the Co^{2+} and Cu^{2+} complexes were recorded with a *Bruker-ESP-380* spectrometer equipped with continuous-flow cryostats for liq. He or for liq. N_2, operating at X-band. The complexes were prepared as $1.25 \cdot 10^{-3}$ M solns. in 1.0M $NaClO_4$, except when indicated. The spectra of $[CoL^1]^-$ (pH 4.03 and 6.62) and $[CoL^2]^-$ (pH 5.88) were recorded at 4 K in aq. soln., and the latter complex was also recorded at 10 K in glycerol/H_2O 1:1. The spectra of $[CuL^1]^-$ were recorded at pH 3.18 (at 127 K) and 6.67 (at 107 and 127 K). For the Cu^{2+}/**2** complexes, the spectra were recorded for the ratio Cu^{2+}/**2** 1:1 at pH values 3.36 and 6.72 and at 100 and 127 K, and for the ratio 2:1 (and 1.9:1), as $1.10 \cdot 10^{-3}$ to $4.50 \cdot 10^{-2}$ M solns. in 1.0M $NaClO_4$, at pH 4.0 at 130 and at 106 and 4 K. Spectra of the 2:1 species were also recorded in H_2O/ethylene glycol 1:1 and in dimethylformamide at 8 K.

Crystal-Structure Determination of [Cu(HL¹)] · 0.5 H₂O. Crystal Data. $C_{16}H_{27}CuN_3O_{8.5}$, M 460.99, triclinic; $a = 8.1426(9)$, $b = 9.2558(9)$, $c = 14.6720(9)$ Å; $\alpha = 101.874(6)$, $\beta = 92.583(7)$, $\gamma = 114.245(9)°$; $V = 976.2(2)$ Å^3; $T = 293(2)$, space group $P\bar{1}$ (no 2), $Z = 2$, $d_c = 1.56$ g cm^{-3}, $\mu = 1.88$ mm^{-1}; $F(000) = 480$. Of the 4430 collected reflections, 3694 were independent ($R_{int} = 0.0569$) and used in the structure solution and refinement.

Data Collection and Processing. Data were collected at r.t. with an *Enraf-Nonius-TURBO-CAD4* apparatus, equipped with a copper rotating anode in the range $3.11 < \theta < 69.9°$. Radiation was monochromated with graphite (λ 1.5415 Å). A crystal with dimensions $0.2 \times 0.2 \times 0.4$ mm^3 was used. Data reduction and an empirical absorption correction were made with MOLEN [46].

Structure Analysis and Refinement. The structure was solved by a combination of *Patterson* and difference *Fourier* synthesis. All non-H-atoms were refined on F^2, with anisotropic thermal parameters. The H-atoms were introduced in idealized positions riding on the parent C-atom. A disordered H_2O molecule was located near special position 0 0.5 0. A disorder model allowing the molecule to be positioned within a circle centered at this position with 0.8 Å radius was found to be better than anisotropically refining the molecule at the special position, $R_1 = 0.0513$ *vs.* $R_1 = 0.0539$. A H-atom located near the position of atom O(6) of a carboxylate moiety was allowed to refine freely. Final R values are: R_1 ($I > 2\sigma I$) = 0.0513, wR_2 ($I > 2\sigma I$) = 0.1268, R_1 (all data) = 0.0695 and wR_2 (all data) = 0.1458. The goodness of fit for 273 refined parameters is $s = 1.09$. Final peak/hole 0.773/ – 0.746 eÅ^{-3}. All the calculations were performed with SHELX86 [47] and SHELX97 [48]. SCHAKAL97 [49] was used for molecular diagrams.

The authors acknowledge Dr. *R. Herrmann* for the helpful discussions and the financial support from *PRAXIS XXI* (Project n. PRAXIS/2/2.1/QUI/316/94).

REFERENCES

[1] R. Bhula, P. Osvath, D. C. Weatherburn, *Coord. Chem. Rev.* **1988**, *91*, 89.
[2] P. V. Bernhardt, G. A. Lawrance, *Coord. Chem. Rev.* **1990**, *104*, 297.
[3] R. M. Izatt, K. Pawlak, J. S. Bradshaw, R. L. Bruening, *Chem. Rev.* **1995**, *95*, 2529.
[4] P. Chaudhuri, K. Wieghardt, *Prog. Inorg. Chem.* **1987**, *35*, 329.
[5] Z. Urbanczyk-Lipkowska, P. Gluzinski, J. W. Krajewski, R. A. Kolinski, A. Kemme, A. Mishnyov, *J. Crystallogr. Spectrosc. Res.* **1989**, *19*, 387.
[6] R. E. Marsh, I. Bernal, *Acta Crystallogr., Sect. B* **1995**, *51*, 300.
[7] Y. Li, *Bull. Chem. Soc. Jpn.* **1996**, *69*, 2513.

[8] T. Sakurai, K. Kobayashi, S. Tsuboyama, Y. Kohno, N. Azuma, K. Ishizu, *Acta Crystallogr., Sect. C* **1983**, *39*, 206.
[9] R. Delgado, J. J. R. Fraústo da Silva, M. C. T. A. Vaz, *Polyhedron* **1987**, *6*, 29; R. Delgado, J. J. R. Fraústo da Silva, M. C. T. A. Vaz, P. Paoletti, M. Micheloni, *J. Chem. Soc.*, *Dalton Trans.* **1989**, 133.
[10] M. F. Cabral, R. Delgado, *Helv. Chim. Acta* **1994**, *77*, 515.
[11] R. Delgado, Y. Sun, R. J. Motekaitis, A. E. Martell, *Inorg. Chem.* **1993**, *32*, 3320.
[12] a) M. Kodama, T. Koike, A. B. Mahatma, E. Kimura, *Inorg. Chem.* **1991**, *30*, 1270; b) M. Kodama, E. Kimura, *Bull. Chem. Soc. Jpn.* **1995**, *68*, 852.
[13] R. Delgado, J. J. R. Fraústo da Silva, *Talanta* **1982**, *29*, 815; S. Chaves, R. Delgado, J. J. R. Fraústo da Silva, *Talanta* **1992**, *39*, 249.
[14] M. T. S. Amorim, R. Delgado, J. J. R. Fraústo da Silva, M. C. T. A. Vaz, M. F. Vilhena, *Talanta* **1988**, *35*, 741.
[15] a) S. Chaves, A. Cerva, R. Delgado, *Polyhedron* **1998**, *17*, 93; b) S. Chaves, A. Cerva, R. Delgado, *J. Chem. Soc., Dalton Trans.* **1997**, 4181.
[16] S. M. Hart, J. C. A. Boeyens, J. P. Michael, R. D. Hancock, *J. Chem. Soc., Dalton Trans.* **1983**, 1601.
[17] J. Costa, R. Delgado, M. G. B. Drew, V. Félix, *J. Chem. Soc., Dalton Trans.* **1998**, 1063.
[18] F. R. Fronczek, V. J. Gatto, C. Minganti, R. A. Schultz, R. D. Gandour, G. W. Gokel, *J. Am. Chem. Soc.* **1984**, *106*, 7244.
[19] K. A. Byriel, L. R. Gahan, C. H. L. Kennard, J. L. Latten, P. C. Healy, *Aust. J. Chem.* **1993**, *46*, 713.
[20] R. D. Hancock, A. E. Martell, *Chem. Rev.* **1989**, *89*, 1875.
[21] A. E. Martell, R. D. Hancock, R. J. Motekaitis, *Coord. Chem. Rev.* **1994**, *133*, 39.
[22] M. G. B. Drew, J. Nelson, S. M. Nelson, *J. Chem. Soc., Dalton Trans.* **1981**, 1685.
[23] L. Alderighi, P. Gans, A. Ienco, D. Peters, A. Sabatini, A. Vacca, *Coord. Chem. Rev.* **1999**, *184*, 311.
[24] C. Bazzicalupi, A. Bencini, A. Bencini, A. Bianchi, F. Corana, V. Fusi, C. Giorgi, P. Paoli, P. Paoletti, B. Valtancoli, C. Zanchini, *Inorg. Chem.* **1996**, *35*, 5540.
[25] I. Bertini, C. Luchinat, *Adv. Inorg. Biochem.* **1984**, *6*, 71.
[26] A. B. P. Lever, 'Inorganic Electronic Spectroscopy', 2nd edn., Elsevier, Amsterdam, 1984.
[27] M. Valko, R. Klement, P. Pelikán, R. Boca, L. Dlhán, A. Böttcher, H. Elias, L. Müller, *J. Phys. Chem.* **1995**, *99*, 137.
[28] A. Bencini, I. Bertini, G. Canti, D. Gatteschi, C. Luchinat, *J. Inorg. Biochem.* **1981**, *14*, 81.
[29] L. Banci, A. Bencini, C. Benelli, D. Gatteschi, C. Zanchini, *Struct. Bonding* **1982**, *52*, 37.
[30] A. Bencini, C. Benelli, D. Gatteschi, C. Zanchini, *Inorg. Chem.* **1979**, *18*, 2526.
[31] J. P. Jesson, *J. Chem. Phys.* **1966**, *45*, 1049.
[32] F. S. Kennedy, H. A. O. Hill, T. A. Kaden, B. L. Vallee, *Biochem. Biophys. Res. Commun.* **1972**, *48*, 1533.
[33] L. Sacconi, F. Mani, A. Bencini, 'Comprehensive Coordination Chemistry', Vol. V, Eds. G. Wilkinson, R. D. Gillard, and J. A. McCleverty, Pergamon Press, 1987, p. 1 – 137.
[34] R. W. Renfrew, R. S. Jamison, D. C. Weatherburn, *Inorg. Chem.* **1979**, *18*, 1584.
[35] L. Y. Martin, C. R. Sperati, D. H. Busch, *J. Am. Chem. Soc.* **1977**, *99*, 2968.
[36] F. Neese, 'Diploma Thesis', University of Konstanz, Germany, June, 1993.
[37] V. Félix, R. Delgado, M. T. S. Amorim, S. Chaves, A. M. Galvão, M. T. Duarte, M. A. A. F. de C. T. Carrondo, I. Moura, J. J. R. Fraústo da Silva, *J. Chem. Soc., Dalton Trans.* **1994**, 3099.
[38] S. Chaves, R. Delgado, M. T. Duarte, J. A. L. Silva, V. Félix, M. A. A. F. de C. T. Carrondo, *J. Chem. Soc., Dalton Trans.* **1992**, 2579.
[39] H. Yokoi, M. Sai, T. Isobe, S. Ohsawa, *Bull. Chem. Soc. Jpn.* **1972**, *45*, 2189.
[40] P. W. Lau, W. C. Lin, *J. Inorg. Nucl. Chem.* **1975**, *37*, 2389.
[41] M. J. Maroney, N. J. Rose, *Inorg. Chem.* **1984**, *23*, 2252.
[42] J. Peisach, W. E. Blumberg, *Arch. Biochem. Biophys.* **1974**, *165*, 691.
[43] T. D. Smith, J. R. Pilbrow, *Coord. Chem. Rev.* **1974**, *13*, 173.
[44] D. M. Duggan, D. N. Hendrickson, *Inorg. Chem.* **1974**, *13*, 2929.
[45] P. Gans, A. Sabatini, A. Vacca, *J. Chem. Soc., Dalton Trans.* **1985**, 1195.
[46] Enraf Nonius, 'MOLEN Data Reduction Software'.
[47] G. M. Sheldrick, *Acta Crystallogr., Sect. A*, **1990**, *46*, 467.
[48] G. M. Sheldrick, 'SHELXL-97', University of Göttingen, Germany, 1997.
[49] E. Keller, 'SCHAKAL97. A Computer Program for the Graphic Representation of Molecular and Crystallographic Models', Krystallogr. Institut der Universität, Freiburg, Germany, 1997.

Received November 17, 1999